

Formulation for Reliable Analysis of Structural Frames

George Corliss (george.corliss@marquette.edu)

Electrical and Computer Engineering, Marquette University

Christopher Foley (chris.foley@marquette.edu)

Civil and Environmental Engineering, Marquette University

R. Baker Kearfott (rbk@louisiana.edu)

Mathematics, University of Louisiana at Lafayette

Abstract. Structural engineers use design codes formulated to consider uncertainty for both reinforced concrete and structural steel design. For a simple one-bay structural steel frame, we survey typical uncertainties and compute an interval solution for displacements and forces. The naive solutions have large over-estimations, so we explore the Mullen-Muhanna element-by-element strategy, scaling, and constraint propagation to achieve tight enclosures of the true ranges for displacements and forces in a fraction of the CPU time typically used for simulations. That we compute tight enclosures, even for large parameter uncertainties used in practice, suggests the promise of interval methods for much larger structures.

Keywords: structural steel frames, partially constrained connections, uncertain parameters, interval arithmetic, element-by-element, constraint propagation.

1. Introduction

Structural engineers have used design codes formulated to consider uncertainty for both reinforced concrete and structural steel design for several decades. The format for these design codes has been termed Load and Resistance Factor Design (LRFD). The LRFD format for structural steel design is founded upon first-order, second-moment reliability theory applied to structural loads and resistances (Cornell, 1969). LRFD-based design rests on the following definition for the probability of structural failure,

$$P_F = P((R - Q) < 0), \quad (1)$$

where

R = a structure's resistance, which is considered a random variable, modeled using a known probability density function (PDF);

Q = the load effect, which is also a random variable with known PDF.

The frequency distribution of the resulting random variable, $R - Q$, allows the definition of a safety margin against structural failure. The probability of failure expressed in Equation (1) is re-phrased as (Ravindra & Galambos, 1978),

$$P_F = P(\ln(R/Q) < 0) .$$

If one knew the probability distribution of $\ln(R/Q)$, determining the probability of failure for the structure would be very easy. Unfortunately, there are several random variables that

contribute to structural resistance as well as load effect. These contributors do not all follow the same PDF's, and the process of characterizing them also is uncertain. In this paper, we use interval arithmetic to compute reliable bounds for structure responses in the presence of uncertain parameters. In section 2, we discuss the nature of the uncertainties and realistic bounds.

The first-order second-moment method approximates the failure of a structure by the safety index (Ravindra & Galambos, 1978),

$$\beta = \frac{\text{mean}(\ln(R/Q))}{\sigma(\ln(R/Q))},$$

where $\sigma(\ln(R/Q))$ is the standard deviation of the natural logarithm of the ratio of resistance to load. In a simplistic sense, the LRFD formulation seeks to define a probability of a failure using an acceptable number of β 's away from mean($\ln(R/Q)$). The acceptable value of β for various structural components is determined using calibration with existing structural systems. In other words, the LRFD design procedures that were proposed, and are currently in use, provide a level of reliability against structural failure that is near that of structures designed using pre-LRFD criteria.

In the discipline of structural engineering, the engineer is often concerned with determining response quantities for which there is very small probability of exceedance. For example, one may be interested in the lateral displacement at the top of the frame shown in Figure 1 for which the probability of exceedance is 0.1%. Since life-safety is involved in design of structural systems, we may desire a very small coefficient of variation in this probabilistic estimate.

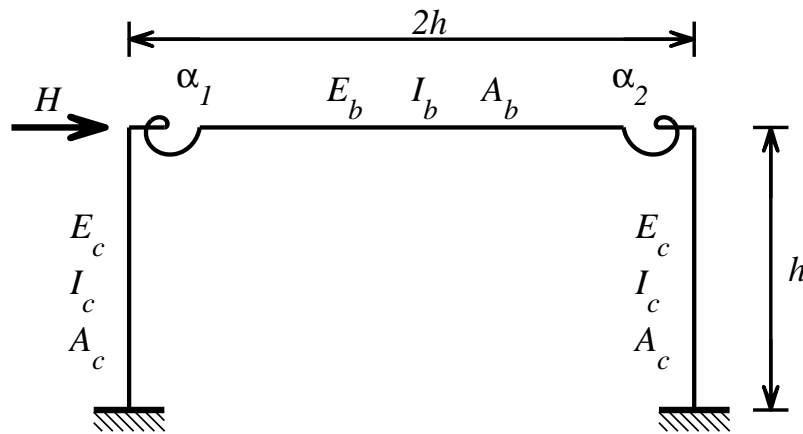


Figure 1. Simple one bay portal frame with partially constrained connections.

Monte-Carlo simulation is a traditional approach for establishing safety indices or probabilities of failure for structural systems. Unfortunately, simulation also includes a level of uncertainty in the results. Better results require more simulations. Soong and Grigoriu

(Soong & Grigoriu, 1993) have shown that the coefficient of variation in an estimated probability \bar{P} can be written as

$$V_{\bar{P}} = \sqrt{\frac{1 - P_{\text{true}}}{N \cdot P_{\text{true}}}}, \quad (2)$$

where P_{true} is the true probability, and N is the number of simulations. Equation (2) can be solved for a required number of simulations using a desired probability and coefficient of variation. If our structural analysis determining the unlikely structural response should have a probability of failure of 0.001 and we need to have a small coefficient of variation in that estimate (e.g., 0.05), then by Equation (2), 399,600 simulations are necessary. That is, nearly 400,000 structural analyses are required to be able to determine structural response for an event with very low probability with high confidence. Other simulation techniques are available, e.g., importance sampling (Melchers, 2001). However, in general, simulation can be a highly expensive tool for understanding uncertainty in structural engineering.

Recent work (Mullen & Muhanna, 1999; Muhanna & Mullen, 2001) introduced intervals as a means for reliably accounting for uncertainty in structural engineering. The present study considers load and resistance uncertainty using interval-based structural analysis. The success of the present work foreshadows additional applications of interval methods in structural engineering to quantify uncertainty in progressive collapse, ground motion analysis, and other highly important endeavors. Furthermore, it is hoped that the interval-based results can be used to *quantify* any error present in structural engineering design as a result of first-order, second-moment reliability-based design methods for complex structures.

2. Development of Intervals for Load and Resistance

Structural loads and resistances frequently are defined using probability density function models for the frequency of occurrence of properties or loading magnitudes characterizing structural behavior. This section assigns intervals of known confidence for cross-sectional properties, loading, material properties, and connection response.

2.1. LATERAL WIND LOADING

The frequency of occurrence of extreme wind speeds is modeled using Fisher-Tippett Type 1 Extreme Value probability distributions (Simiu et al., 1978). To demonstrate the process, a hypothetical extreme wind record is used to generate wind speed intervals and then a wind pressure interval suitable for structural analysis. The mean peak wind speed (assumed here to be for 3-second gusts) and standard deviation for a 19-year record are

$$\bar{V}_{3\text{-sec}} = 62.7 \text{ mph} \quad \sigma_{3\text{-sec}} = 8.63 \text{ mph.}$$

The PDF assumed allows one to compute peak wind speeds and confidence levels associated with those speeds that include sampling error due to the limited number of years for

which data is available. Buildings are often assumed to have service life spans of 50 years. If one is willing to accept that the wind speed used for design has a 5% chance of being exceeded in 50 years, one is establishing a 1,000 year mean recurrence interval wind. In other words, there is a 0.1% chance that the wind speeds used for design will be exceeded in any given year.

Given a number of data points in a peak wind speed record and a known probability density function describing frequency of occurrence, an estimate of the N -year peak wind speed and standard deviation in the estimate that includes sampling errors can be determined using (Simiu et al., 1978)

$$\widehat{V}_{3\text{-sec}}^N = \bar{V}_{3\text{-sec}} + \sigma_{3\text{-sec}}(y - 0.5772) \frac{\sqrt{6}}{\pi}, \text{ and} \quad (3)$$

$$\text{SD} \left(\widehat{V}_{3\text{-sec}}^N \right) = [1.645 + 1.462(y - 0.5772) + 1.1(y - 0.5772)^2]^{0.5} \frac{0.78 \sigma_{3\text{-sec}}}{\sqrt{n}}, \quad (4)$$

where

$$y = -\ln \left[-\ln \left(1 - \frac{1}{N} \right) \right];$$

N = mean recurrence interval (years) for peak wind in question;

$\widehat{V}_{3\text{-sec}}^N$ estimated value of the N -year, peak 3-second wind;

$\text{SD} \left(\widehat{V}_{3\text{-sec}}^N \right)$ = standard deviation in the estimate for the N -year 3-second wind;

$\bar{V}_{3\text{-sec}}^N$ = sample mean for 3-second peak winds measured;

$\sigma_{3\text{-sec}}$ = sample standard deviation for 3-second peak winds measured;

n = sample size in years.

We define an interval for peak wind speeds using Equations (3) and (4). Our target for the design analysis is to set a 0.1% probability that the peak winds used to assign lateral wind load magnitudes will be exceeded. As mentioned earlier, this equates to a 1,000 year mean recurrence interval wind, or $N = 1,000$ years. The estimated value of the 1,000-year wind and the standard deviation in the estimate based upon the 19-year sample size are computed using equations (3) and (4):

$$\widehat{V}_{3\text{-sec}}^N = 105.29 \text{ mph, and } \text{SD} \left(\widehat{V}_{3\text{-sec}}^N \right) = 11.450 \text{ mph.} \quad (5)$$

Using the values given in Equation (5), we can assign intervals for peak 3-second wind speeds in a highly flexible manner. For example, assume that we wish to have two standard deviations of confidence in the peak 3-second wind speed. The interval of wind speeds corresponding to this is

$$82.39 \leq \widehat{V}_{3\text{-sec}}^N \leq 128.19 \text{ mph} \quad \text{or} \quad \widehat{V}_{3\text{-sec}}^N = 105.29 \pm 22.9 \text{ mph.} \quad (6)$$

This wind speed interval can be interpreted as follows. There is a 99.9% confidence that the peak wind speed will be less than or equal to 105.29 mph. However, this estimate is based

upon limited peak wind speed data. Therefore, the error in the estimate that bounds this level of confidence in the expected peak wind has been defined as two standard deviations above and below the estimate. Thus, one has two standard deviations of confidence that the 1,000 year wind will not be exceeded. One can then say there is an acceptably low probability of the wind speed exceeding 128.19 mph.

Building codes (ASCE, 2002) use peak wind speeds of known averaging time to convert these speeds into design pressures for building structures. The expression to carry out this conversion is based upon the classical work of Bernoulli (ASCE, 2002),

$$q = 0.00256 \cdot K_z \cdot K_{zt} \cdot K_d \cdot V^2 \cdot I . \quad (7)$$

For the sake of simplicity, we assume

$$\begin{aligned} I &= 1.0 \text{ (importance factor)} \\ K_d &= 0.85 \text{ (directionality factor)} \\ K_{zt} &= 1.0 \text{ (topographic effect factor)} \\ K_z &= 0.70 \text{ (height factor)}. \end{aligned}$$

Using the peak wind speed interval of Equation (6), the corresponding interval for the peak pressures computed using Equation (7) is

$$10.34 \leq q^{\text{peak}} \leq 25.03 \text{ psf} \quad \text{or} \quad q^{\text{peak}} = 17.685 \pm 7.345 \text{ psf}.$$

If we assume a structural system layout that contains the portal frame shown in Figure 1, we can compute an interval for the peak applied lateral loads at the top of the frame. If we assume that the height of the frame is 12 feet and the lateral load resisting portal frames are 50 feet apart, the peak lateral loads are expected to lie within

$$3,102 \leq H \leq 7,509 \text{ lbs} \quad \text{or} \quad H = 5,305.5 \pm 2,203.5 \text{ lbs}.$$

2.2. MEMBER MATERIAL AND CROSS-SECTIONAL PROPERTIES

The loading is only one aspect to the uncertainty in structural engineering problems. Material and cross-sectional properties for component members within the structure are also subject to uncertainty. The portal frame shown in Figure 1 contains one beam member and two column members.

The beam members are W18×35, with mean cross-sectional area and second moment of area (AISC, 2001)

$$A_b = 10.3 \text{ in}^2 \quad \text{and} \quad I_b = 510 \text{ in}^4 .$$

(Cecen, 1974) and (Ravindra & Galambos, 1978) suggest statistical data for describing the fabrication-related variation in A_b and I_b :

$$\begin{aligned} \mu_F &= 1.0 \text{ (mean)} \\ V_F &= 0.05 \text{ (coefficient of variation)}, \end{aligned}$$

which lead to

$$\sigma_F = 0.05 \text{ (standard deviation)}.$$

Cross-sectional properties are assumed to follow a normal statistical distribution (Ravindra & Galambos, 1978). Therefore, two standard deviations above and below the mean ensure approximately 95% confidence that the parameters lie within the stated interval. Therefore, mid-point and interval radii are

$$A_b = 10.3 \pm 1.03 \text{ in}^2 \quad \text{and} \quad I_b = 510 \pm 51 \text{ in}^4.$$

Columns are W10×49 members, with mean cross-section properties (AISC, 2001)

$$A_c = 14.4 \text{ in}^2 \quad \text{and} \quad I_c = 272 \text{ in}^4.$$

Using the same argument as that used for the beams above, intervals that consider uncertainty in the cross-sectional properties of the column members are

$$A_c = 14.4 \pm 1.44 \text{ in}^2 \quad \text{and} \quad I_c = 272 \pm 27.2 \text{ in}^4.$$

Uncertainty in material properties (e.g., material modulus) are often described using a normally distributed random variable (Ravindra & Galambos, 1978) with mean

$$E = 29,000,000 \text{ lb/in}^2.$$

(Cecen, 1974) and (Ravindra & Galambos, 1978) suggest the following statistical data for describing the variation in E :

$$\begin{aligned} \mu_F &= 1.0 \text{ (mean), and} \\ V_F &= 0.06 \text{ (coefficient of variation),} \end{aligned}$$

which lead to

$$\sigma_F = 0.06 \text{ (standard deviation).}$$

Two standard deviations above and below the mean ensure approximately 95% confidence that the true values of the parameters lie within the stated interval. Therefore, interval mid-point and radius are

$$E = 29,000,000 \pm 3,480,000 \text{ lb/in}^2.$$

2.3. CONNECTIONS

The framework considered in Figure 1 also includes connections at the beam ends that are assumed to be partially restrained. These connections will not force the 90 degree angle made between beams and columns to remain 90 degrees after deformation of the frame laterally. These are often modeled as nonlinear springs. However, for simplicity and demonstration of concept, we assume the springs are linear.

Physical testing is used to determine the stiffness and strength characteristics of structural steel connections found in real structures. Unfortunately, there have been very few studies undertaken to quantify the statistical variation in connection response. (Deierlein et al., 1991) report examination of statistical parameters for a typical structural steel connection classified as partially-restrained. This connection is the top-and-seat angle connection with web cleats (TSAW).

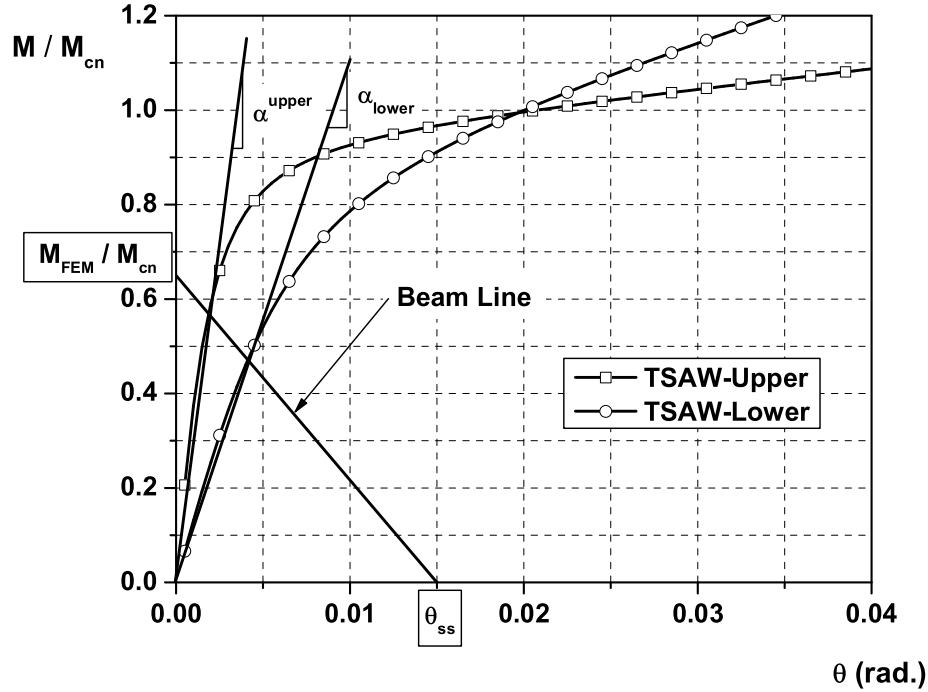


Figure 2. Beam-line approach for linearizing connection stiffness.

Uncertainty in nonlinear response of the TSAW connections was found to be adequately described using a normally distributed random variable (Deierlein et al., 1991). Linearization of connection response for purposes of structural analysis is commonly accomplished using the beam-line approach. The beam-line approach is schematically illustrated in Figure 2. The approach is well documented, and details will not be presented here. We assume that repeated loading and unloading of the connections results in shake-down to the linear connection stiffness established using the beam-line.

The connection stiffness uncertainty used in the present study is generated using the upper and lower-bound nonlinear connection curves for the TSAW connections discussed in (Deierlein et al., 1991). These two curves (shown in Figure 2) constitute boundaries for which there is 95% confidence that the expected connection behavior is captured. This corresponds to plus or minus two standard deviations from the mean. The connection curves are normalized with respect to the connection capacity, M_{cn} . For the present study, $M_{cn} = 0.4M_{pb}$, where M_{pb} is the plastic moment capacity of the connected beam.

Using the beam-line concept and the W18×35 beam member, the linear connection stiffness magnitudes corresponding to the upper- and lower-bound connection curves are

$$\alpha^{\text{upper}} = 403,965 \text{ k} \cdot \text{in}/\text{rad}$$

$$\alpha^{\text{lower}} = 150,957 \text{ k} \cdot \text{in}/\text{rad}.$$

The midpoint and radius for the connection stiffness 95% confidence interval are

$$\alpha = 277,461 \pm 126,504 \text{ k} \cdot \text{in/rad} .$$

For simplicity, we assume that the connection of the columns to the foundation is rigid, although the present formulation can account for variability in connection response at the foundation.

3. Frame Components

We model each component of the frame shown in Figure 1 in an object-oriented manner, following the notation of (Hibbeler, 2002). We describe the structural components in an object-oriented manner, foreshadowing both the mathematical analysis to follow and the implementation in computer code.

3.1. COMPONENT: MEMBER

Let \cdot_N denote values at the near node and \cdot_F denote values at the far node. We use $r_{N\hat{z}}$ instead of Hibbeler's $d_{N\hat{z}}$ to reserve $d_{N\hat{z}}$ for 3-dimensional frames.

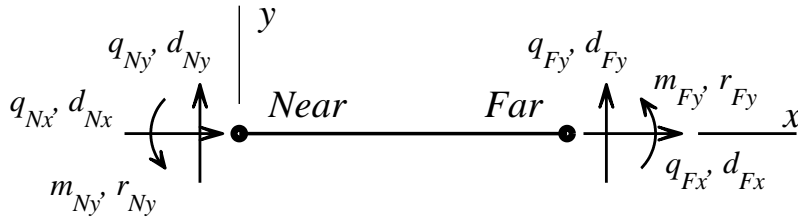


Figure 3. Member local forces, moments, displacements, and rotations (after Hibbeler 2002).

Attributes (in local ($\hat{\cdot}$) or global coordinates):

- Displacements: $d_{N\hat{x}}, d_{N\hat{y}}, d_{F\hat{x}}, d_{F\hat{y}}$ (local) or $d_{Nx}, d_{Ny}, d_{Fx}, d_{Fy}$ (global)
- Rotations: $r_{N\hat{z}}, d_{F\hat{z}}$ (local) or r_{Nz}, d_{Fz} (global)
- Forces: $q_{N\hat{x}}, q_{N\hat{y}}, q_{F\hat{x}}, q_{F\hat{y}}$ (local) or $q_{Nx}, q_{Ny}, q_{Fx}, q_{Fy}$ (global)
- Moments: $m_{N\hat{z}}, m_{F\hat{z}}$ (local) or m_{Nz}, m_{Fz} (global)

Properties: Frame-member stiffness equation:

$$\begin{bmatrix} \frac{AE}{L} & 0 & 0 & \frac{-AE}{L} & 0 & 0 \\ 0 & \frac{12EI}{L^3} & \frac{6EI}{L^2} & 0 & \frac{-12EI}{L^3} & \frac{6EI}{L^2} \\ 0 & \frac{6EI}{L^2} & \frac{4EI}{L} & 0 & \frac{-6EI}{L^2} & \frac{2EI}{L} \\ \frac{-AE}{L} & 0 & 0 & \frac{AE}{L} & 0 & 0 \\ 0 & \frac{-12EI}{L^3} & \frac{-6EI}{L^2} & 0 & \frac{12EI}{L^3} & \frac{-6EI}{L^2} \\ 0 & \frac{6EI}{L^2} & \frac{2EI}{L} & 0 & \frac{-6EI}{L^2} & \frac{4EI}{L} \end{bmatrix} \begin{bmatrix} d_{N\hat{x}} \\ d_{N\hat{y}} \\ r_{N\hat{z}} \\ d_{F\hat{x}} \\ d_{F\hat{y}} \\ r_{F\hat{z}} \end{bmatrix} = \begin{bmatrix} q_{N\hat{x}} \\ q_{N\hat{y}} \\ m_{N\hat{z}} \\ q_{F\hat{x}} \\ q_{F\hat{y}} \\ m_{F\hat{z}} \end{bmatrix}$$

or $\kappa(A, E, L, \mathbf{d} - \mathbf{q}) = \mathbf{k}'\mathbf{d} - \mathbf{q} = 0$. Typical values for frame parameters and applied loading are (see §2):

$$\begin{aligned} E_b = E_c &= 29,000,000 \pm 3,480,000 \text{ lbs/in}^2 \text{ (12\%)} \\ I_b &= 510 \pm 51 \text{ in}^4; I_c = 272 \pm 27.2 \text{ in}^4 \text{ (10\%)} \\ A_b &= 10.3 \pm 10.3 \text{ in}^2; A_c = 14.4 \pm 1.44 \text{ in}^2 \text{ (10\%)} \\ H &= 5,305.5 \pm 2,203.5 \text{ lbs (41.6\%)} \\ \alpha &= 277,461,000 \pm 126,504,000 \text{ lb-in/rad (45.6\%)} \\ L_c &= 144 \text{ in}; L_b = 2L_c . \end{aligned} \tag{8}$$

Local coordinates are transformed to global coordinates by transformation matrices. For each member, let $\lambda_x = \cos \theta$ and $\lambda_y = \cos \phi$, so that $\lambda_x^2 + \lambda_y^2 = 1$. Let

$$T = \begin{bmatrix} \lambda_x & \lambda_y & 0 & 0 & 0 & 0 \\ -\lambda_y & \lambda_x & 0 & 0 & 0 & 0 \\ 0 & 0 & 1 & 0 & 0 & 0 \\ 0 & 0 & 0 & \lambda_x & \lambda_y & 0 \\ 0 & 0 & 0 & -\lambda_y & \lambda_x & 0 \\ 0 & 0 & 0 & 0 & 0 & 1 \end{bmatrix} .$$

Then $TT^T = T^T T = \text{Identity}$.

3.2. COMPONENT: END

An “End” is an end of a Member (or a Joint). The Ends define the topology of the structure. Our End corresponds somewhat to the usual notion of a Node, except that we use “Connections” to join Members and Joints.

Attributes (in global coordinates):

- Displacements: d_x, d_y
- Rotations: r_z
- Forces: q_x, q_y, q_{Ex}, q_{Ey}

- Moments: m_z, m_{Ez} ,

where \cdot_E denotes externally applied forces and moments.

Properties:

- Can be incident with two or more Members and Joints
- Displacements d_x, d_y , and r_z are equal for all Members and Joints incident on an End
- Forces $q_{Ex} + q_x, q_{Ey} + q_y$, and moments $m_{Ez} + m_z$ each sum to zero for all Members and Joints incident on an End

3.3. COMPONENT: JOINT

Attributes (in local or global coordinates):

- Displacements: $d_{N\hat{x}}, d_{N\hat{y}}, d_{F\hat{x}}, d_{F\hat{y}}$
- Rotations: $r_{N\hat{z}}, d_{F\hat{z}}$
- Forces: $q_{N\hat{x}}, q_{N\hat{y}}, q_{F\hat{x}}, q_{F\hat{y}}$
- Moments: $m_{N\hat{z}}, m_{F\hat{z}}$

Properties:

- Length = 0
- Joins one Member to another
- Global displacements d_x are equal for incident End and Member
- Global displacements d_y are equal for incident End and Member
- Global forces q_x are equal for incident End and Member
- Global forces q_y are equal for incident End and Member
- Local rotations and moments satisfy

$$\begin{bmatrix} \alpha & -\alpha \\ -\alpha & \alpha \end{bmatrix} \begin{bmatrix} r_{N\hat{z}} \\ r_{F\hat{z}} \end{bmatrix} = \begin{bmatrix} m_{N\hat{z}} \\ m_{F\hat{z}} \end{bmatrix}$$

4. Assembly

Following the usual practice (e.g., (Hibbeler, 2002)), we assemble a linear system corresponding to the structure in Figure 4, identifying equal displacements and summing appropriate forces, to ensure that both equilibrium and compatibility of displacements are satisfied.

Columns 1 – 5:

$$\begin{bmatrix} \frac{12E_c I_c}{L_c^3} + \frac{A_b E_b}{L_b} & 0 & \frac{6E_c I_c}{L_c^2} & 0 & 0 \\ 0 & \frac{A_c E_c}{L_c} + \frac{12E_b I_b}{L_b^3} & 0 & \frac{6E_b I_b}{L_b^2} & \frac{6E_b I_b}{L_b^2} \\ \frac{6E_c I_c}{L_c^2} & 0 & \frac{4E_c I_c}{L_c} + \alpha & -\alpha & 0 \\ 0 & \frac{6E_b I_b}{L_b^2} & -\alpha & \frac{4E_b I_b}{L_b} + \alpha & \frac{2E_b I_b}{L_b} \\ 0 & \frac{6E_b I_b}{L_b^2} & 0 & \frac{2E_b I_b}{L_b} & \frac{4E_c I_c}{L_c} + \alpha \\ -\frac{A_b E_b}{L_b} & 0 & 0 & 0 & 0 \\ 0 & -\frac{12E_b I_b}{L_b^3} & 0 & -\frac{6E_b I_b}{L_b^2} & -\frac{6E_b I_b}{L_b^2} \\ 0 & 0 & 0 & 0 & -\alpha \end{bmatrix}$$

Columns 6 – 8:

$$\begin{bmatrix} -\frac{A_b E_b}{L_b} & 0 & 0 \\ 0 & -\frac{12E_b I_b}{L_b^3} & 0 \\ 0 & 0 & 0 \\ 0 & -\frac{6E_b I_b}{L_b^2} & 0 \\ 0 & -\frac{6E_b I_b}{L_b^2} & -\alpha \\ \frac{A_b E_b}{L_b} + \frac{12E_c I_c}{L_c^3} & 0 & \frac{6E_c I_c}{L_c^2} \\ 0 & \frac{12E_b I_b}{L_b^3} + \frac{A_c E_c}{L_c} & -\frac{6E_b I_b}{L_b^2} \\ \frac{6E_c I_c}{L_c^2} & -\frac{6E_b I_b}{L_b^2} & \frac{4E_c I_c}{L_c} + \alpha \end{bmatrix} \begin{bmatrix} d2_x \\ d2_y \\ r2_z \\ r5_z \\ r6_z \\ d3_x \\ d3_y \\ r3_z \end{bmatrix} = \begin{bmatrix} H \\ 0 \\ 0 \\ 0 \\ 0 \\ 0 \\ 0 \\ 0 \end{bmatrix} \quad (9)$$

The global stiffness matrix K given by Equation (9) has condition number $\text{cond}(K) = 4.7\text{e}+04$. Solving using mid-point values of parameters given in Equation (8) yields

	Displacement d_x	Displacement d_y	Rotation r_z
Connection 2	0.15356843	0.00033236	-0.00096285
Connection 3	0.15102784	-0.00033236	-0.00094313
Connection 5			-0.00045995
Connection 6			-0.00044556
	Force q_x	Force q_y	Moment m_z
Connection 1	-2670.516	-963.856	245019.992
Connection 4	-2634.984	963.856	241381.602

The ranges given in Equation (8) for the parameters in this system suggest using interval arithmetic (Moore, 1966; Moore, 1979; Neumaier, 1990). Interval arithmetic computes with

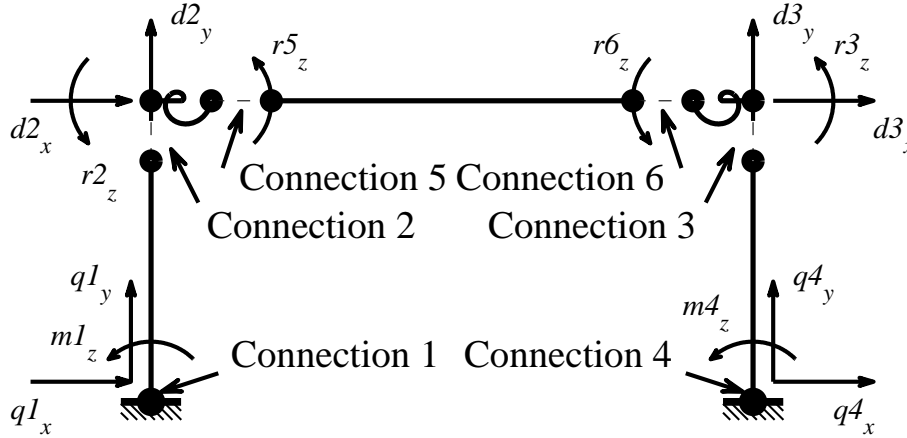


Figure 4. Element-by-element assembly.

guaranteed lower and upper bounds. It accounts for uncertain parameters and roundoff errors in computation. Our problem has uncertain parameters, and the condition number of $4.7e+04$ for even such a simple frame suggests that roundoff is a potential concern, especially as we scale to larger structures.

In interval arithmetic, operations are defined set-wise. That is, if $[a] = [\underline{a}, \bar{a}]$ and $[b] = [\underline{b}, \bar{b}]$ are intervals,

$$[a] + [b] = \{a + b : a \in [a], b \in [b]\} = [\underline{a} + \underline{b}, \bar{a} + \bar{b}].$$

In a practical implementation, the additions of the endpoints are done using IEEE outwardly directed rounding. Other operations and elementary functions are defined similarly.

Initially, we use intervals of uncertainty 1% of those given in Equation (8). For example, instead of using $H = 5,305.5 \pm 2,203.5$ lbs, we use $5,305.5 \pm 22.035$ lbs. We form the global stiffness matrix K given by Equation (9) using interval values of the parameters and solve.

Table I gives the naive interval solution of the one-bay frame problem. The column “Float” contains the floating point solutions to the system whose coefficients are given by the midpoints of the parameter intervals. The column “Interval” contains the solution computed by an interval linear equation solver applied to Equation (9) with interval coefficients. The column “Midpoint \pm Radius” contains the same intervals as the column “Interval,” except that they are expressed in a midpoint \pm radius form, rather than an endpoint form.

The “Interval” solutions contain the true values, but narrower enclosures are better than wide ones. Naive interval computations, as we have done here, are prone to overestimation. For the rows labeled “Tight:,” we solved the 2^{10} extremal individual problems formed by taking lower and upper bounds of the intervals for each of the 10 parameters in this system. Since the system is linear, the solution to **any** combination of parameter values taken from the respective intervals must lie in the convex hull of the solutions to the extremal problems. This is **not** simulation since parameter values are chosen not at random but as extremal values. The column “Relative overestimation” is the width of the “Interval”

Table I. Naive interval solution of the one-bay frame problem.

Disp.	Float	Interval True range	Midpoint \pm Radius Rel. overest.
$d2_x$	0.153568	[0.09375783, 0.21337873]	0.1535683 \pm 0.05981
	Tight:	[0.15237484, 0.15476814]	76.34%
$d2_y e+3$	0.332364	[0.19060424, 0.47412283]	0.3323635 \pm 0.1418
	Tight:	[0.32940418, 0.33533906]	83.52%
$r2_z e+3$	-0.962852	[-1.3531968, -0.57250484]	-0.9628508 \pm 0.3903
	Tight:	[-0.97085151, -0.95490139]	79.42%
$r5_z e+3$	-0.459955	[-0.6557609, -0.26414725]	-0.4599541 \pm 0.1958
	Tight:	[-0.4638112, -0.45611532]	83.47%
$r6_z e+3$	-0.445563	[-0.64100045, -0.2501251]	-0.4455628 \pm 0.1954
	Tight:	[-0.44930811, -0.4418354]	86.05%
$d3_x$	0.151028	[0.091230936, 0.21082444]	0.1510277 \pm 0.0598
	Tight:	[0.14985048, 0.15221127]	77.62%
$d3_y e+3$	-0.332364	[-0.47412283, -0.19060424]	-0.3323635 \pm 0.1418
	Tight:	[-0.33533906, -0.32940418]	83.52%
$r3_z e+3$	-0.943133	[-1.3330326, -0.55323186]	-0.9431322 \pm 0.3899
	Tight:	[-0.95100335, -0.93531196]	81.02%

solution not contained in the “Tight” solution, scaled by the “Float” solution, and expressed as a percentage. Given that intervals are guaranteed to enclose the true answers, the goal is to compute enclosures with as little over-estimation as possible.

We observe

- “Interval” solutions contain the approximate “Float” solutions and the “Tight” solutions, illustrating the claim of enclosure.
- “Interval” solutions are hopelessly pessimistic. The relative over-estimations are too large to have practical utility.
- We used parameter uncertainties of 1% of the intervals given in Equation (8). If we use 4%, the interval linear solver fails because the global stiffness matrix includes matrices that are singular since we have perturbed by 4% elements of a matrix with condition $4.7e+04$.
- In the Matlab environment we used, the “Interval” solution takes 1,200 times the CPU time for the approximate solution. That CPU cost should be compared with the CPU cost of 400,000 simulation runs, which do not provide the reliability of the interval results.

Rather than conclude interval arithmetic is not practical, we conclude that we must be more clever in its application. The rest of this paper leads us through a sequence of increasingly

sophisticated formulations until we are able to solve a system equivalent to Equation (9) with parameter uncertainties 1.5 times the widths of the intervals given in Equation 8.

5. Element-by-Element

The excessive overestimation in Table I comes from the “dependency problem” common in evaluation of expressions in interval arithmetic. For example, if we take $[x] = [-1, 2]$, Table II shows that even for some simple expressions, mathematically equivalent expressions do not give the same interval results because the set-wise definition of interval operations does not recognize that the same interval appearing in different contexts must be the same value. The interval operator $-$ cannot distinguish $[x] - [x]$, which equals 0, from $[x] - [y]$ with $[x] = [y]$, which does not. In general, expressions in which each variable appears only once (Single Use Expression, SUE) are evaluated with no over-estimation. In naive Gaussian elimination with back substitution applied to a system of order n , the coefficient $K_{1,1}$ appears in the symbolic expression for $d1_x$ a total of $\mathcal{O}(n^2)$ times, hardly a Single Use Expression.

Table II. Overestimation from dependencies in expressions with $[x] = [-1, 2]$.

$x - x$	$[-3, 3]$	vs.	0	$[0, 0]$
$x * x$	$[-2, 4]$	vs.	x^2	$[0, 4]$

(Mullen & Muhanna, 1999) suggested an element-by-element approach for structural engineering trusses. Instead of a finite element formulation, they introduced extra variables and added extra equations to the system to reduce the interval dependencies. We apply the Mullen-Muhanna element-by-element approach to frames. The difference is in the way we assemble the global stiffness matrix. From an object-oriented perspective, “End” becomes an inherent attribute of the Member and Joint classes. Each Member and Joint in the structure becomes its own block in the global stiffness matrix, with both displacements and forces at each end as unknowns. “Node” becomes a new Connector class, adding rows to the global stiffness matrix rows expressing that adjacent ends have identical displacements and rotations and that forces and moments at each connection sum to zero.

Joint J_1 global stiffness matrix:

$$\begin{aligned}
 d3_x - d4_x &= 0; & d3_y - d4_y &= 0 \\
 \alpha r 3_z - \alpha r 4_z - m 3_z &= 0 \\
 q 3_x + q 4_x &= 0; & q 3_y + q 4_y &= 0 \\
 -\alpha r 3_z + \alpha r 4_z - m 4_z &= 0 .
 \end{aligned}$$

Member M_1 global stiffness matrix:

$$\begin{bmatrix} \frac{12E_c I_c}{L_c^3} & 0 & -\frac{6E_c I_c}{L_c^2} & -\frac{12E_c I_c}{L_c^3} & 0 & -\frac{6E_c I_c}{L_c^2} \\ 0 & \frac{A_c E_c}{L_c} & 0 & 0 & -\frac{A_c E_c}{L_c} & 0 \\ -\frac{6E_c I_c}{L_c^2} & 0 & \frac{4E_c I_c}{L_c} & \frac{6E_c I_c}{L_c^2} & 0 & \frac{2E_c I_c}{L_c} \\ -\frac{12E_c I_c}{L_c^3} & 0 & \frac{6E_c I_c}{L_c^2} & \frac{12E_c I_c}{L_c^3} & 0 & \frac{6E_c I_c}{L_c^2} \\ 0 & -\frac{A_c E_c}{L_c} & 0 & 0 & \frac{A_c E_c}{L_c} & 0 \\ -\frac{6E_c I_c}{L_c^2} & 0 & \frac{2E_c I_c}{L_c} & \frac{6E_c I_c}{L_c^2} & 0 & \frac{4E_c I_c}{L_c} \end{bmatrix} \begin{bmatrix} d1_x \\ d1_y \\ r1_z \\ d2_x \\ d2_y \\ r2_z \end{bmatrix} - \begin{bmatrix} q1_x \\ q1_y \\ m1_z \\ q2_x \\ q2_y \\ m2_z \end{bmatrix} = 0 .$$

Members M_2 and M_3 and Joint J_2 are handled similarly.

Connector C_2 (we'll see C_1 later) connecting Member M_1 with Joint J_1 requires equality of incident displacements:

$$[d2_x, d2_y, r2_z]^T - [d3_x, d3_y, r3_z]^T = 0 ,$$

and that incident forces sum to zero:

$$q2_x + q3_x = H; \quad q2_y + q3_y = 0; \quad m2_z + m3_y = 0 .$$

This is the first non-zero right hand side so far. Connector C_3 connecting Joint J_1 with Member M_2 requires equality of incident displacements and that incident forces sum to zero:

$$\begin{aligned} [d4_x, d4_y, r4_z]^T - [d5_x, d5_y, r5_z]^T &= 0 \\ [q4_x + q5_x, q4_y + q5_y, m2_z + m3_y]^T &= 0 . \end{aligned}$$

Connectors C_4 and C_5 are handled similarly. Connector C_1 fixes Member M_1 to the ground, and connector C_6 fixes Member M_3 :

$$[d1_x, d1_y, r1_z]^T = 0; \quad [d10_x, d10_y, r10_z]^T = 0 .$$

For simplicity of exposition, we retain the last two sets of equations corresponding to displacements and rotations known to be zero. The solution of the element-by-element global stiffness system using intervals of uncertainty 1% of those given in Equation (8) in interval arithmetic is shown in Table III. The condition number is 1.2e+17. This condition number leads one to suspect that, in exact arithmetic, the matrix may be exactly singular.

With such a large condition number, it is surprising that we get essentially the same answers as before, but it is disappointing that the interval radii are not significantly smaller than for the naive interval solution shown in Table I. However, there are many common terms in many of the matrix coefficients. For example, see the global stiffness matrix for Member M_1 . We can factor them out and take advantage of subdistributivity.

Table III. Interval solution the Mullen-Muhanna element-by-element approach.

Disp.	Float	Interval True range	Midpoint \pm Radius Rel. overest.
$d2_x$	0.153568	[0.09246203, 0.21467453]	0.1535683 \pm 0.06111
	Tight:	[0.15237484, 0.15476814]	78.02%
$d2_y e+3$	0.332364	[0.18751797, 0.4772091]	0.3323635 \pm 0.1448
	Tight:	[0.32940418, 0.33533906]	85.38%
$r2_z e+3$	-0.962852	[-1.361667, -0.56403468]	-0.9628508 \pm 0.3988
	Tight:	[-0.97085151, -0.95490139]	81.18%
$r5_z e+3$	-0.459955	[-0.66002154, -0.25988661]	-0.4599541 \pm 0.2001
	Tight:	[-0.4638112, -0.45611532]	85.32%

6. Subdistributivity

In interval arithmetic, we have

$$a(b + c) \subseteq ab + ac \quad (\text{subdistributivity}).$$

For example, $[-1, 2] * ([4, 5] + [-3, -2]) = [-3, 6] \subseteq [-1, 2] * [4, 5] + [-1, 2] * [-3, -2]$. Hence, to get tighter enclosures, we want to extract common factors whenever possible, as suggested by (Mullen & Muhanna, 1999) for trusses.

For example, consider equations 9 and 12 from the Joint J_1 stiffness matrix and equations 21 and 24 from the Joint J_2 stiffness matrix. Let $d_{61} := r3_z - r4_z$ and $d_{62} := r7_z - r8_z$. Then

$$\text{Eq. 9 \& 21: } \alpha d_{61} - m3_z = 0; \quad \alpha d_{62} - m7_z = 0$$

$$\text{Eq. 12: } \alpha d_{61} + m4_z = 0 \text{ or } m3_z + m4_z = 0$$

$$\text{Eq. 24: } \alpha d_{62} + m8_z = 0 \text{ or } m7_z + m8_z = 0$$

$$\text{Eq. 61 \& 62: } r3_z - r4_z - d_{61} = 0; \quad r7_z - r8_z - d_{62} = 0 .$$

Next, consider the Member M_1 global stiffness matrix:

$$\begin{bmatrix} \frac{12E_c I_c}{L_c^3} & 0 & -\frac{6E_c I_c}{L_c^2} & -\frac{12E_c I_c}{L_c^3} & 0 & -\frac{6E_c I_c}{L_c^2} \\ 0 & \frac{A_c E_c}{L_c} & 0 & 0 & -\frac{A_c E_c}{L_c} & 0 \\ -\frac{6E_c I_c}{L_c^2} & 0 & \frac{4E_c I_c}{L_c} & \frac{6E_c I_c}{L_c^2} & 0 & \frac{2E_c I_c}{L_c} \\ -\frac{12E_c I_c}{L_c^3} & 0 & \frac{6E_c I_c}{L_c^2} & \frac{12E_c I_c}{L_c^3} & 0 & \frac{6E_c I_c}{L_c^2} \\ 0 & -\frac{A_c E_c}{L_c} & 0 & 0 & \frac{A_c E_c}{L_c} & 0 \\ -\frac{6E_c I_c}{L_c^2} & 0 & \frac{2E_c I_c}{L_c} & \frac{6E_c I_c}{L_c^2} & 0 & \frac{4E_c I_c}{L_c} \end{bmatrix} \begin{bmatrix} d1_x \\ d1_y \\ r1_z \\ d2_x \\ d2_y \\ r2_z \end{bmatrix} - \begin{bmatrix} q1_x \\ q1_y \\ m1_z \\ q2_x \\ q2_y \\ m2_z \end{bmatrix} = 0 .$$

Let

$$\begin{aligned} d_{63} &:= \frac{A_c E_c}{L_c} (d1_y - d2_y) & d_{65} &:= \frac{2E_c I_c}{L_c} (r1_z + r2_z) \\ d_{64} &:= \frac{6E_c I_c}{L_c^2} (d1_x - d2_x) & d_{66} &:= \frac{2E_c I_c}{L_c} r1_z, \end{aligned}$$

which leads to a considerably simpler system

$$\begin{aligned} \text{Eq. 1 : } & \frac{2}{L_c} d_{64} - \frac{3}{L_c} d_{65} - q1_x = 0 \\ \text{Eq. 2 : } & d_{63} - q1_y = 0 \\ \text{Eq. 3 : } & -d_{64} + d_{65} + d_{66} - m1_z = 0 \\ \text{Eq. 4 \& 5 : } & q1_x + q2_x = 0; \quad q1_y + q2_y = 0 \\ \text{Eq. 6 : } & -d_{64} + 2d_{65} - d_{66} - m2_z = 0 \\ \text{Eq. 63: } & d1_y - d2_y - \frac{L_c}{A_c E_c} d_{63} = 0 \\ \text{Eq. 64: } & d1_x - d2_x - \frac{L_c^2}{6E_c I_c} d_{64} = 0 \\ \text{Eq. 65: } & r1_z + r2_z - \frac{L_c}{2E_c I_c} d_{65} = 0 \\ \text{Eq. 66: } & r1_z - \frac{L_c}{2E_c I_c} d_{66} = 0. \end{aligned}$$

The global stiffness matrices for Members M_2 and M_3 are handled similarly. The solution of the element-by-element global stiffness system using intervals of uncertainty 1% of those given in Equation (8) in interval arithmetic is shown in Table IV. $\text{Cond}(K) = 1.2\text{e}+17$.

Table IV. Interval solution the Mullen-Muhanna element-by-element approach.

Disp.	Float	Interval True range	Midpoint \pm Radius Rel. overest.
$d2_x$	0.153568	[0.15206288, 0.15507492]	0.1535689 \pm 0.001506
	Tight:	[0.15237484, 0.15476814]	0.40%
$d2_y\text{e}+3$	0.332364	[0.32918317, 0.33554758]	0.3323654 \pm 0.003182
	Tight:	[0.32940418, 0.33533906]	0.13%
$r2_z\text{e}+3$	-0.962852	[-0.97485786, -0.95084958]	-0.9628537 \pm 0.012
	Tight:	[-0.97085151, -0.95490139]	0.84%
$r5_z\text{e}+3$	-0.459955	[-0.46757208, -0.45234116]	-0.4599566 \pm 0.007615
	Tight:	[-0.4638112, -0.45611532]	1.63%

These results in Table IV are about two orders of magnitude tighter than the interval element-by-element method shown in Table III. Further, we can solve the system with relative uncertainty 1.5 times the intervals of uncertainty given in Equation (8), compared with 0.01 before. That allows us to handle practical engineering tolerances.

So far, we have replicated the work of Mullen and Muhanna, except applied to frames instead of trusses. Their work speaks of factoring the stiffness equations, although they might not have done so in exactly the same way we have done it. To further reduce interval over-estimation, we try scaling the equations and applying constraint propagation.

7. Scaling

In traditional numerical analysis, seeing solution components varying over eight orders of magnitude and a condition number of $1.2e+17$ is a warning sign. Let's try scaling variables to have similar magnitudes.

It appears that scaling all forces by the input force $H = 5305.5$ would be good. We cannot do that by simply replacing $H = 5305.5$ by $H = 1$ because H appears only on the right hand side, so that replacement would have no effect on $\text{cond}(K)$.

In the right hand side, we can replace the interval $[H]$ by its midpoint \tilde{H} and then multiply the solution by $[H]/\tilde{H} = [1 - \delta, 1 + \delta]$. That replaces one of the interval parameters by a degenerate interval in the computation of the solution. The result is a very slight further reduction in the uncertainties of the solution.

Next, in each equation, we replace each variable force ($q1_x, \dots$) by force/ \tilde{H} . Each of the intermediate variables d_{61}, \dots, d_{74} introduced in the Subdistributivity section are of the same order as forces, so we scale them by \tilde{H} , too. Hence in the global stiffness matrix, each coefficient of a force or a newly introduced intermediate variable is multiplied by \tilde{H} , unless all of the terms of that equation are in the scaled set. That reduces $\text{cond}(K)$ from about $1.7e+17$ to $2.8e+08$ and yields a further reduction in the widths the Mullen-Muhanna results of Table IV, as shown in Table V.

Table V. Interval solution using scaled element-by-element approach with parameter uncertainties 1% of those in Equation (8).

Disp.	Float	Interval True range	Midpoint \pm Radius Rel. overest.
$d2_x$	0.153568	[0.15294597, 0.15419182]	0.1535689 ± 0.0006229
	Tight:	[0.1531698, 0.15396904]	0.29%
$d2_y e+3$	0.332364	[0.33111682, 0.33361393]	0.3323654 ± 0.001249
	Tight:	[0.3311227, 0.33360764]	0.004%
$r2_z e+3$	-0.962852	[-0.96945816, -0.95624927]	-0.9628537 ± 0.006604
	Tight:	[-0.96583881, -0.95988319]	0.75%
$r5_z e+3$	-0.459955	[-0.46515166, -0.45476159]	-0.4599566 ± 0.005195
	Tight:	[-0.46141645, -0.45849491]	1.62%

Table VI shows the solution to the same system as Table V, except that we use the practical parameter uncertainties given in Equation (8). If we multiply the uncertainties given in Equation (8) by 1.7, we get solution enclosures shown in Table VII. In either case,

we can compute bounds, but bounds are quite over-estimated, and they include values of the wrong sign, an observation which leads us to consider constraint propagation.

Table VI. Interval solution using scaled element-by-element approach with parameter uncertainties from Equation (8).

Disp.	Float	Interval True range	Midpoint \pm Radius Rel. overest.
$d2_x$	0.153568	[0.022924888, 0.29366922]	0.1582971 \pm 0.1354
	Tight:	[0.12130751, 0.20804041]	119.8%
$d2_y e+3$	0.332364	[0.11407836, 0.57891094]	0.3464947 \pm 0.2324
	Tight:	[0.21526742, 0.47234932]	62.51%
$r2_z e+3$	-0.962852	[-2.5286276, 0.55857565]	-0.985026 \pm 1.544
	Tight:	[-1.4124783, -0.73502904]	250.3%
$r5_z e+3$	-0.459955	[-1.7359689, 0.77691797]	-0.4795255 \pm 1.256
	Tight:	[-0.6216869, -0.3157181]	479.8%

Table VII. Interval solution using scaled element-by-element approach with parameter uncertainties 1.7 times of those in Equation (8).

Disp.	Float	Interval True range	Midpoint \pm Radius Rel. overest.
$d2_x$	0.153568	[-2.4422952, 2.7778163]	0.1677605 \pm 2.61
	Tight:	[0.10506254, 0.29253671]	3277%
$d2_y e+3$	0.332364	[-3.726848, 4.4766635]	0.3749077 \pm 4.102
	Tight:	[0.12406102, 0.59793831]	2326%
$r2_z e+3$	-0.962852	[-33.038469, 30.980172]	-1.029148 \pm 32.01
	Tight:	[-2.2934663, -0.62850325]	6476%
$r5_z e+3$	-0.459955	[-27.257812, 26.220056]	-0.5188781 \pm 26.74
	Tight:	[-0.76558971, -0.18556419]	11500%

CPU times for the 58×58 interval solution shown in Tables V - VII are about 2,000 times the CPU time required to solve the approximate 8×8 system of Equation (9) with midpoint values of the parameters. The figure of 2,000 times can reasonably be compared with the nearly 400,000 simulation runs to achieve even comparable confidence intervals. Nonetheless, the cost of the interval computation is at least partially due to the Matlab programming environment in which these experiments were performed. Direct coding with a language with an interval datatype, even if that datatype is implemented with operator overloading, probably would result in an order-of-magnitude speedup of the interval computations. These results also point to a need for a quality suite of interval sparse matrix routines.

8. Constraint Propagation

The solution enclosures in Tables VI and VII show large uncertainty, and they include non-physical values, e.g., compression rather than tension. The stiffness matrix is close to singular. Constraint propagation can help, because we can always intersect with physically known constraints.

Constraint propagation originated in the field of logic programming. (Van Hentenryck et al., 1997) is an excellent explanation of constraint propagation in an interval context. The idea is best illustrated by an example. Suppose we seek roots in $[-4, 4]$ of $f(x) = x^2 + x - 5 = 0$. Solve for the linear occurrence of x , $x = 5 - x^2$. On the right, substitute $x = [-4, 4]$: $x = 5 - [-4, 4]^2 = 5 - [0, 16] = [-11, 5]$. That is, if a root x^* of $x^2 + x - 5 = 0$ lies in the interval $[-4, 4]$, then it must also lie in the interval $[-11, 5]$, not an especially helpful result.

Next, solve for the quadratic occurrence of x , $x = \pm\sqrt{5 - x}$. On the right, substitute $x = [-4, 4]$: $x = \pm\sqrt{5 - [-4, 4]} = \pm\sqrt{[1, 9]} = [-3, -1] \cup [1, 3]$. That is, if a root x^* of $x^2 + x - 5 = 0$ lies in the interval $[-4, 4]$, then it must also lie in the interval $[-3, -1]$ or the interval $[1, 3]$. Further iteration of $x = \sqrt{5 - x}$ from $x = [1, 3]$ yields

$$\begin{aligned} x = & [1.41421356237309, 2.00000000000000] \\ & [1.73205080756887, 1.89361728911280] \\ & [1.76249332222485, 1.80774699347866] \\ & [1.78668771936265, 1.79930727719730] \\ & [1.78904799343189, 1.79257141577047] \\ & [1.79092953078269, 1.79191294614669] , \end{aligned}$$

which is converging to the root $x^* = 1.79128784747792$.

Constraint propagation can be viewed as discarding candidate solutions that are infeasible with respect to already known information. It is Gauss-Seidel iteration, except that we solve each equation for each variable. Constraint propagation is especially attractive for sparse systems, such as ours.

To describe a generic constraint propagation algorithm for a linear system $Ax = b$, we denote the set of unknowns by $x = (x_i)$ and use $A_jx = b_j$, for a single equation.

Loop until converged

 Loop for each j

 In principle, consider equation j : $A_jx = b_j$

 For each variable x_i which appears in $A_jx = b_j$, “solve” for x_i

 Let $[x_i] := [x_i] \cap$ expression for x_i evaluated with $[x]$

 If the intersection is empty, there is no solution. STOP

 If any intersection is smaller, the solution is converging

There are various strategies for choosing the order of iteration of equations and variables and many implementation details, which we ignore here.

Using the the practical parameter uncertainties given in Equation (8) and starting with the solution enclosures shown in Table VI, we get the results shown in Table VIII. Constraint

propagation tightened the enclosure of $d2_y$, but did not improve significantly on the quality of the interval solution.

Table VIII. Constraint propagation starting with solutions from Table VI.

Disp.	Float	Interval True range	Midpoint \pm Radius Rel. overest.
$d2_x$	0.153568	[0.022924888, 0.29366922]	0.1582971 ± 0.1354
	Tight:	[0.12130751, 0.20804041]	119.8%
$d2_y e+3$	0.332364	[0.17032525, 0.57868876]	0.374507 ± 0.2042
	Tight:	[0.21526742, 0.47234932]	45.52%
$r2_z e+3$	-0.962852	[-2.5286276, 0.55857565]	-0.985026 ± 1.544
	Tight:	[-1.4124783, -0.73502904]	250.3%
$r5_z e+3$	-0.459955	[-1.7359689, 0.77691797]	-0.4795255 ± 1.256
	Tight:	[-0.6216869, -0.3157181]	479.8%

Starting with $[0.5, 1.5]$ times the approximate solution using midpoint values, using **no** interval system solver, and five iterations of constraint propagation, we get the results shown in Table IX. We achieve relative over-estimations that are comparable to the relative uncertainties in the parameters, in spite of a condition number of $2.8e+08$.

Table IX. Constraint propagation starting with $[0.6, 1.4]$ times the approximate solution using midpoint values.

Disp.	Float	Interval True range	Midpoint \pm Radius Rel. overest.
$d2_x$	0.153568	[0.076784216, 0.23035265]	0.1535684 ± 0.07678
	Tight:	[0.12130751, 0.20804041]	43.52%
$d2_y e+3$	0.332364	[0.166182, 0.49854599]	0.332364 ± 0.1662
	Tight:	[0.21526742, 0.47234932]	22.65%
$r2_z e+3$	-0.962852	[-1.4442773, -0.48142577]	-0.9628515 ± 0.4814
	Tight:	[-1.4124783, -0.73502904]	29.64%
$r5_z e+3$	-0.459955	[-0.68993206, -0.22997735]	-0.4599547 ± 0.23
	Tight:	[-0.6216869, -0.3157181]	33.48%

9. Conclusions and Future Directions

To the structural engineering community, along with the work of (Mullen & Muhanna, 1999) and (Muhanna & Mullen, 2001), we have demonstrated the feasibility of interval techniques. One set of interval computations can guarantee to enclose the displacements, rotations, forces, and moments that could be observed from any combination of values of

cross-sectional properties, loading, material properties, and connections, even for quite large uncertainties. In subsequent work, we will extend these techniques to non-linear behaviors and to larger structures.

To the interval community, we have demonstrated a variety of techniques to achieve relatively tight enclosures of the solution to a realistic (although small) problem, even in the face of parameter uncertainties over 40%. We used an element-by-element approach, which adds equations specifying that two variables are the same, rather than simplifying by identifying them with the same variable. We used symbolic rearrangement, scaling of the equations, and constraint propagation. In subsequent work, to handle larger systems, we will explore sparsity-preserving preconditioning, more effective and efficient constraint propagation, and branch-and-bound-like strategies for subdividing the ranges of wide interval-valued parameters.

References

- AISC. Manual of Steel Construction, Load and Resistance Factor Design, 3rd Edition. American Institute of Steel Construction, Chicago, Ill., 2001.
- ASCE. Minimum design loads for buildings and other structures, ASCE 7-02. American Society of Civil Engineers, Reston, Va., 2002.
- H. Cecen. Computer-aided, reliability based, optimum design of multi-story steel frames. Master's thesis, Washington University, St. Louis, Mo., 1974.
- C.A. Cornell. A probability-based structural code. *Journal of the American Concrete Institute*, 66(12), December 1969.
- Gregory G. Deierlein, S.-H. Hsieh, Y.-J. Shen, and John F. Abel. Nonlinear analysis of steel frames with semi-rigid connections using capacity spectrum approach. Technical Report NCEER-91-0008, National Center for Earthquake Engineering Research, SUNY at Buffalo, Buffalo, NY, 1991.
- Russell C. Hibbeler. *Structural Analysis, Fifth Edition*. Prentice Hall, Englewood Cliffs, NJ, 2002.
- Robert E. Melchers. *Structural Reliability Analysis and Prediction, 2nd Edition*. John Wiley and Sons, New York, 2001.
- Ramon E. Moore. *Interval Analysis*. Prentice Hall, Englewood Cliffs, NJ, 1966.
- Ramon E. Moore. *Methods and Applications of Interval Analysis*. SIAM, Philadelphia, PA, 1979.
- Rafi L. Muhanna and Robert L. Mullen. Uncertainty in mechanics problems – interval-based approach. *Journal of Engineering Mechanics*, 2001.
- Robert L. Mullen and Rafi L. Muhanna. Bounds of structural response for all possible loading conditions. *Journal of Structural Engineering*, 1999.
- Arnold Neumaier. *Interval Methods for Systems of Equations*. Cambridge University Press, Cambridge, 1990.
- Mayasandra K. Ravindra and Theodore V. Galambos. Load and resistance factor design for steel. *Journal of the Structural Division*, 104, 1978.
- Emil Simiu, Jacques Bietry, and James J. Filliben. Sampling errors in estimation of extreme winds. *Journal of the Structural Division*, 104(3), 1978.
- T.T. Soong and Mircea Grigoriu. *Random Vibration of Mechanical and Structural Systems*. Prentice Hall, Englewood Cliffs, NJ, 1993.
- Pascal Van Hentenryck and Laurent Michel and Yves Deville. *Numerica: A Modeling Language for Global Optimization*. MIT Press, Cambridge, Mass., 1997.